Materials and Structures (2015) 48:797–814
DOI 10.1617/s11527-014-0516-z

ORIGINAL ARTICLE

Statistical justification of Model B4 for drying and autogenous shrinkage of concrete and comparisons to other models

Mija H. Hubler · Roman Wendner · Zdeněk P. Bažant

Received: 5 June 2014 / Accepted: 19 December 2014 / Published online: 8 January 2015

Abstract The shrinkage prediction part of Model B4 presented in the preceding paper is here statistically justified by optimal fitting of the new NU database containing 1050 test curves and by statistical comparisons with the existing shrinkage prediction models. Rather than attempting a point-wise constitutive model for free shrinkage, Model B4 predicts the average shrinkage of cross sections of long members, which are affected by nonuniform residual stresses relaxing due to creep and microcracking. The main improvement in Model B4, which extends the 1995 Model B3 (a RILEM recommendation), is that separate formulae are given for: (1) the drying shrinkage, which represents most of the shrinkage observed in normal concretes of high water–cement ratios, and (2) for the autogenous shrinkage, which has a different physical mechanism and is important for modern high-performance concretes with admixtures, additives and low water–cement ratios. The effect of elevated temperature on the shrinkage rate is captured through an equivalent accelerated time based on activation energy. Model B4 is statistically calibrated by the new NU database of laboratory shrinkage tests through a sequential optimization procedure which isolates different physical behaviors. The new shrinkage equations are shown to match the time curves of individual shrinkage tests well, and fit the database with minimum error. Statistics of extensive comparisons with Model B3 and with the models of various engineering societies, including those of ACI and *fib*, document a superior fit of the new model to the database.

Keywords Shrinkage · Concrete · Prediction · Database · Calibration · Statistical comparisons

M. H. Hubler · R. Wendner
Civil and Evironmental Engineering, Northwestern University, Evanston, IL, USA

Present Address:
M. H. Hubler
Civil and Environmental Engineering, Massachusettes Institute of Technology, Cambridge, USA

Present Address:
R. Wendner
Christian–Doppler Laboratory on Life−Cycle Robustness of Fastening Technology, Institute of Structural Engineering, University of Natural Resources and Life Sciences, Vienna, Austria

Z. P. Bažant (✉)
Civil and Mechanical Engineering and Materials Science, Northwestern University, Evanston, IL, USA
e-mail: z-bazant@northwestern.edu

1 Introduction

A preceding paper [1] presented Model B4 for creep and shrinkage prediction, which extends and refines the previous Model B3 (1995 RILEM Recommendation). It introduces a separation of drying and

autogenous shrinkage, which is important for modern high-performance concretes. A second preceding paper [2] outlined the method of statistical optimization of the fits of an extensive experimental database [3]. This paper provides a statistical justification of the shrinkage prediction formulae presented in [1] and a comparison with the formulae of other engineering societies [4–7, 8, 9], while the companion paper [10] provides justification for the creep formulation.

2 Why a theoretically based rather than empirical formula is needed?

First it should be noted that the existing shrinkage data from laboratory tests give no information on shrinkage durations exceeding 6 years, and are scant for durations exceeding 1.5 years, which represent only 20 % of the available curves. Except for the tests of thin cement paste wafers, most data do not extend to the final plateau, which is the most important property. Also, the existing data are extremely scant for structural member thicknesses exceeding 0.15 m, and are unavailable in a form usable for empirical fitting for >0.5 m. A sufficient number of consistent tests that are statistically representative, are performed in a controlled environment and include concretes both with and without admixtures, is required for empirical fitting purposes.

Yet, large span bridges and very tall buildings contain members of thickness >1 m, for which, based on the well verified diffusion model for drying, the drying has halftimes >30 years and terminates at >300 years. For thickness >0.15 m the drying at constant environment does not terminate in less than 10 years.

Similar to creep [10], shrinkage formulae obtained by intuitive extrapolation of the existing data cannot be trusted. Unlike creep, the multi-decade data on bridges and other structures are, unfortunately, too complex and too scattered for extracting the long-term shrinkage properties. So, for shrinkage, a theoretical extrapolation in time and thickness is, at present, the only way.

The theoretical basis for drying shrinkage can be briefly summarized in the following points:

(1) As a consequence of diffusion theory, an increase of thickness D scales the shrinkage curve horizontally, rather than vertically, i.e., decelerates the shrinkage evolution, with the halftime, τ_{sh}, being proportional to D^2 (the result is a horizontal shift of the curve of shrinkage strain ϵ_{sh} versus $\log(t-t_0)$ by $2\log(D/D_0)$ (D_0 = reference thickness, $t-t_0$ = duration of drying);
(2) the diffusion theory (linear as well as nonlinear [11]) requires that the shrinkage must initially evolve as $\sqrt{t-t_0}$, and
(3) the halftime to be proportional to permeability.
(4) The diffusion theory also yields the cross-section shape effect on the shrinkage halftime,
(5) gives a change of environmental humidity that scales the shrinkage approximately vertically, and
(6) requires the shrinkage to have a final asymptotic bound, ϵ_∞, which is approached approximately exponentially.
(7) Increasing the age at drying exposure stiffens the microstructure against the compression caused by surface tensions and thus scales down the shrinkage curve, approximately in proportion to $E(t_0+\tau_{sh})$, but
(8) at the same time reduces moisture diffusivity, which scales the shrinkage curve horizontally.
(9) According to the activation energy theory, the effect of constant elevated temperature on shrinkage is captured by acceleration of time, particularly the reduction of halftime. Model B4 (as well as B3) follows all these theoretical requirements.

The mathematical description of shrinkage (as well as drying creep) is greatly complicated by the fact that the current design practice demands the average shrinkage properties of the whole cross section of a structural member (as discussed, e.g., in [7, 12, 13]). This makes it impossible to reveal the magnitude and distribution of shrinkage stress and cracking strain over the cross section. A constitutive (or point-wise) equation relating the rate of free shrinkage strain to the rate of pore humidity would be not only more realistic but also much simpler. But it would require: (a) a structural design based on three-dimensional (3D) analysis of stresses, diffusion and cracking, and (b) a complex identification of the shrinkage law from shrinkage test data based on inverse 3D finite element analysis of test specimens, which would be a preposterous task in the case of a large database with thousands of test curves.

For accurate modeling of complex situations such as time variable environmental humidity and temperature, a rate-type modeling of shrinkage, as well as creep, is required. While the creep compliance can easily be converted to a rate-type creep law, as long as the principle of superposition applies [14], for shrinkage such a conversion is more hypothetical although it has been made using some plausible hypotheses [15]. Application of the present model requires the environmental conditions to be constant or randomly fluctuating with an almost constant mean (and a period shorter than τ_{sh}), which is usually true of weather.

3 Brief overview of B4 shrinkage model

The full B4 shrinkage model is presented in [1] along with a calculation example. Example curves for the shrinkage model are shown in Fig. 1. Briefly, the main equations are:

$$\text{Autogenous shrinkage: } \epsilon_{au}(\tilde{t},\tilde{t}_0) = \epsilon_{au\infty}[1+(\tau_{au}/(\tilde{t}+\tilde{t}_0))^{\alpha}]^{r_t}, \quad \alpha = r_\alpha\left(\frac{w/c}{0.38}\right), \tag{1}$$

$$\text{Drying shrinkage: } \epsilon_{sh}(\tilde{t},\tilde{t}_0) = \epsilon_{sh\infty}(\tilde{t}_0)k_h S(\tilde{t}), \tag{2}$$

$$\text{Halftime: } \tau_{sh} = \tau_0(k_s D)^2, \text{effective thickness } D = 2V/S, \tag{3}$$

$$\text{Total shrinkage: } \epsilon_{sh,total}(\tilde{t},\tilde{t}_0) = \epsilon_{sh}(\tilde{t},\tilde{t}_0) + \epsilon_{au}(\tilde{t},\tilde{t}_0), \tag{4}$$

where $\epsilon_{au\infty}, \tau_{au}, r_\alpha, \epsilon_{sh\infty}, k_h, \tau_0$, and k_s are parameters defined in [1]. The major difference from Model B3, the predecessor of B4, and the main innovation, is the separation of shrinkage into a sum of drying and autogenous shrinkage; Eq. (1). Autogenous shrinkage is here defined as the shrinkage of sealed specimens, i.e., at no moisture exchange. It results from volume changes during chemical reactions and the accompanying self-desiccation. The applicable range of temperatures and humidities has been extended, compared to Model B3. The effect of density and stiffness of the aggregate on the shrinkage halftime and the final value has been captured. Except for the mass density of concrete, all the B4 composition parameters are expressed in dimensionless form, which is an advantage compared to B3 and other models.

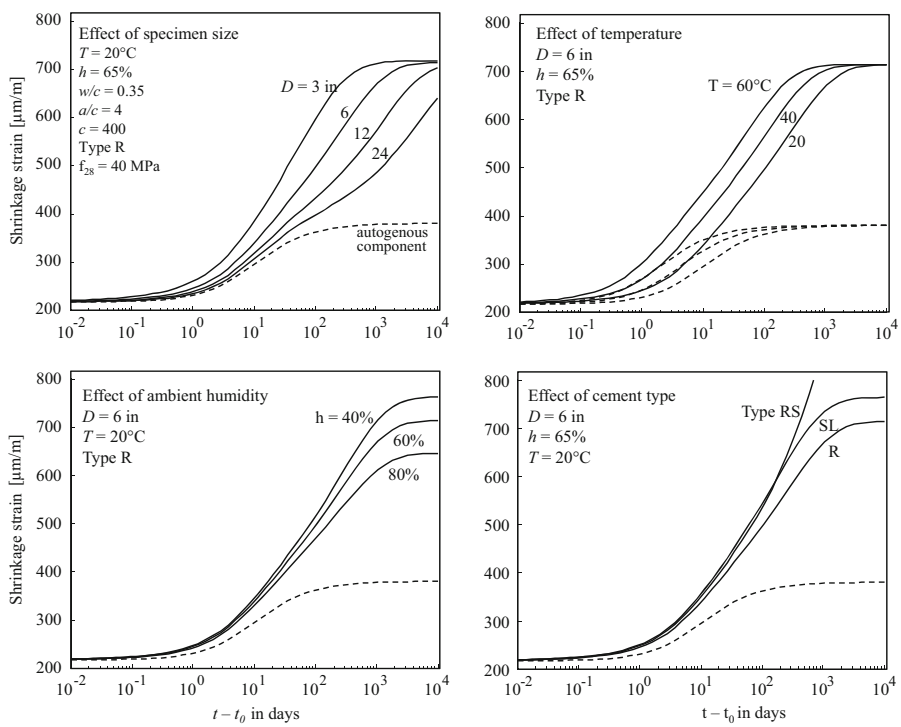

Fig. 1 Typical shrinkage curves given by Model B4, showing the effect of specimen size, temperature, ambient humidity, and cement type

The mean 28-day compressive strength $\bar{f}_{28}$ of concrete is not used in Model B4 because it is strongly correlated to the water–cement ratio w/c. The effect of various binders is treated separately, and is *not* part of the w/c ratio. Various additives undergo some degree of hydration, but this depends on their interactions with other additives and cement, and thus cannot be lumped into one w/b (water–binder) ratio. The following section on additives and admixtures addresses these interactions in more detail and describes them through various empirical relations, such as that listed in [4] (note that if the dependence on strength were used simultaneously with w/c, the optimization problem would become ill-conditioned because these two parameters are strongly correlated).

An alternative simpler model, labeled B4s, has nevertheless also been developed. This model uses solely $\bar{f}_{28}$, instead of all the composition parameters. It is useful for preliminary design when the concrete composition has not yet been decided. B4s can, on the average, fit the database almost as well as Model B4, but it does not allow the designer to estimate directly the effect of changes in concrete composition, which can be large.

Figure 1 presents the B4 predictions of the total shrinkage and the autogenous part of shrinkage for a typical concrete composition as function of size D, ambient humidity h and temperature T, and cement type. It is important to note that the default parameters that are given for Model B4 (as well as Model B4s) are calibrated by fitting the entire shrinkage database and thus they cannot provide a perfect description for a specific concrete. Nonetheless, it will be shown in this paper, by suitable statistical means, that the chosen formulation and time functions are also capable of capturing accurately a specific concrete. Model B4, like its predecessor B3 or the model in *fib* Model Code 2010, is formulated on a cross-section level for beam or plate type analysis. Thus, these models are intended to approximate the average cross-section behavior. This requires several simplifications, some of which will be discussed in detail in the following sections.

4 Model form verification by fitting individual shrinkage curves of broad enough range

The correctness of the shape of the shrinkage curves of any model cannot be verified by fitting the entire database because the scatter due to differences between concretes is far too large, obfuscating the curve shape. The shape can be verified only by the ability to fit individual shrinkage curves of a duration long enough to cover the initial shrinkage and the approach to the final asymptotic value.

For the model form verification, shrinkage measurements taken from [16, 17] are useful. They are the only curves that reveal, in a logarithmic time plot, both the initial straight line of slope 1/2 and an approach to the final asymptotic shrinkage value. The initial slope is dictated by diffusion theory and may be verified by [18–20]. To verify the effect of environmental humidity, use [17, 18, 21–23]; for ambient temperature, use [24–26]; for specimen size, use [19, 27], and for the age at exposure to environment, use [16, 20, 28].

5 Effects of additives, admixtures and aggregates

Within the theoretical framework outlined, the effect of various additives and admixtures on the shrinkage behavior was studied. While some admixtures such as silica fume and air-entraining agents primarily affect the microstructure of concrete, and thus can be captured by a re-calibration of the basic diffusion based formulation, others lead to chemical volume changes and self-desiccation. The latter effect is especially pronounced in high strength concretes, which are notorious for significant self-desiccation caused by loss of free water consumed by hydration. The pore humidity decrease during self-desiccation directly causes shrinkage but also reduces the pore humidity gradient, which retards the rates of drying and of drying shrinkage.

The chemical shrinkage, which is due to low w/c made possible by admixtures, not only causes volume reduction, observed as shrinkage, but also decreases pore humidity. Further complications arise from the diverse admixtures and reactive additives used in modern concretes (e.g., superplasticizer, water reducer and silica fume), which have interdependent opposing or attenuating effects.

Some studies [29] showed that, in combination with the aggregate type effect, the 28-day shrinkage can be changed by up to 400×10^{-6}. The density of rock aggregate appears to have the greatest effect on the shrinkage halftime, the elastic modulus and the final shrinkage, which can be explained by a simple

mechanical model. The aggregate density also affects the effective permeability of concrete. The magnitude of shrinkage is roughly proportional to the material compliance (inverse of stiffness) and, in consequence, also to the contributing aggregate compliance. This dependence is captured in B4 through empirically obtained correction factors $k_{\tau a}$ and $k_{\epsilon a}$, which scale the shrinkage halftime, τ_{sh} and the final shrinkage, ϵ_{∞}, respectively.

6 Total and drying shrinkage shrinkage data

The parameters of the B4 shrinkage model were statistically calibrated by optimizing the fit of the full NU database [3] without compromising the ability to closely fit the individual shrinkage curves. The database contains 1217 shrinkage curves of specimens exposed to a drying environment. They represent the total shrinkage, which is here considered to be the sum of drying shrinkage and autogenous shrinkage. The database also contains 417 curves of autogenous shrinkage, observed on sealed specimens. Among these data there are 177 shrinkage tests in which both the total and autogenous shrinkages were measured. By subtracting them one could get 177 curves of 'pure' drying shrinkage, but the subtraction would be an unproven hypothesis and, therefore, such derived curves have not been used in data fitting.

There is a lack of consensus on the effect of each admixture or additive. This is largely because the market is continuously evolving and no testing standard exists. Nevertheless there are exceptions. One is the tests of Brooks [33–35], in which the superplasticizer is consistently shown to reduce short-term shrinkage, and in particular the autogenous component. Based on [34, 36, 37], the blast furnace slag increases the long-term shrinkage, especially in the case of a high w/c ratio. Silica fume increases both the short-term and long-term shrinkage, and in particular the long-term slope of the shrinkage curve in log-time [34, 38–43]. Tests by Buil and Archer [44], as well as de Larrard [45], indicate the long-term autogenous shrinkage to be twice as large as it is for normal concrete. Low doses of fly ash show no effect on shrinkage [36], but a replacement of between 25 and 50 % of the cement results in an increase of autogenous shrinkage, while a replacement above 50 % reduces autogenous shrinkage compared to normal concrete [46]. Viscosity agents are consistently seen to increase shrinkage [47]. The water reducers and retarders [34, 47], which are the most popular admixtures, however show no consistent trends.

To incorporate the available information on admixtures and their interactions for each data set, a classification system was introduced. Correlation studies were performed between input data containing admixtures and the observed shrinkage measurements. These studies revealed the magnitude and functional form of the deviations due to the presence of admixtures as compared to the shrinkage prediction curve for normal concrete. Data subsets were then created relating the dosages of each admixture and/or combinations of admixtures to parameters introducing these deviations into the prediction equation. The number of subsets introduced to capture the effects of low or high dosages of admixtures depended on the availability of data and the quality of the overall fit resulting from such an introduction. Additionally, for each admixture, the aforementioned observations by various experimenters were taken into account in selecting parameter subsets related to the microstructure and mechanisms.

Therefore, after the formula for the composition effect on autogenous shrinkage has been identified from the database, the tests of shrinkage in a drying environment have been fitted assuming a contribution, whether major or minor, of the autogenous shrinkage as predicted from this formula. This is a major difference from all previous studies, in which the autogenous shrinkage contribution to drying shrinkage tests has not been separated.

7 Autogenous shrinkage data

Formulas for autogenous shrinkage, all of exponential decay form, were proposed by Jonasson and Hedlund [48] and Tazawa [39, 49], and recommended in RILEM [50] and CEB-FIP [51]. The key similarities among these equations is their dependence on the w/c (water–cement) or w/b (water–binder) ratio, cement type, and compressive strength of the concrete. Since the mechanism causing autogenous shrinkage, comprising a multitude of chemical reactions, is a microscale mechanism still not sufficiently clarified, the goal is a simple conservative estimate with the fewest parameters. Because the amount of reactants is finite autogenous shrinkage must approach a final asymptotic value.

Table 1 Admixture dependent parameter scaling factors for shrinkage

Admixture class (% of c)	$\times\tau_{cem}$	$\times\epsilon_{au,cem}$	$\times r_{\epsilon w}$	$\times r_{\alpha}$
Re (>0.5), Fly (≤15)	6.00	0.58	0.50	2.60
Re (>0.5, ≤0.6), Fly (≤15)	2.00	0.43	0.59	3.10
Re (>0.5, ≤0.6), Fly (>15, ≤30)	2.10	0.72	0.88	3.40
Re (>0.5, ≤0.6), Fly (>30)	2.80	0.87	1.60	5.00
Re (>0.6), Fly (<15)	2.00	0.26	0.22	0.95
Re (>0.6), Fly (>15, ≤30)	2.10	1.10	1.10	3.30
Re (>0.6), Fly (>30)	2.10*	1.10	0.97	4.00
Fly (≤15), Super (≤5)	0.32	0.71	0.55	1.71
Fly (≤15), Super (>5)	0.32*	0.55	0.92	2.30
Fly (>15, ≤30), Super (≤5)	0.50	0.90	0.82	1.25
Fly (>15, ≤30), Super (>5)	0.50*	0.80	0.80	2.81
Fly (>30), Super (>5)	0.63	1.38	0.00	1.20
Fly (>30), Super (>5)	0.63*	0.95	0.76	3.11
Super (≤5), Silica (≤8)	6.00	2.80	0.29	0.21
Super (≤5), Silica (>8)	3.00	0.96	0.26	0.71
Super (>5), Silica (≤8)	8.00	1.95	0.00	1.00
Silica (≤8)	1.90	0.47	0.00	1.20
Silica (>8)	2.60	0.82	0.00	1.20
Silica (>18)	1.00	1.50	5.00	1.00
AEA (≤0.05)	2.30	1.10	0.28	0.35
AEA (>0.05)	0.44	4.28	0.00	0.36
WR (≤2)	0.50	0.38	0.00	1.90
WR (>2, ≤3)	6.00	0.45	1.51	0.30
WR (>3)	2.40	0.40	0.68	1.40

* Lacking data, assumed

Sensitivity studies using the NU database revealed the strongest effects of the water–cement and aggregate–cement ratios of each mix. Autogenous shrinkage begins right after mixing but what is of interest for mechanics is only the autogenous shrinkage after the moment of set.

A number of time functions were compared against the experimental data. Optimizing the fits with Eq. (1), the following empirical formulae for the parameters of the final autogenous shrinkage and autogenous shrinkage halftime have been identified [1]:

$$\epsilon_{au\infty} = -\epsilon_{au,cem}\left(\frac{a/c}{6}\right)^{r_{\epsilon a}}\left(\frac{w/c}{0.38}\right)^{r_{\epsilon w}} \quad (5)$$

$$\tau_{au} = \tau_{au,cem}\,\text{days}\left(\frac{\text{w/c}}{0.38}\right)^{\text{r}_{\tau\text{w}}} \quad (6)$$

For the autogenous shrinkage, the admixtures and reactive additives affect the reaction rate, expressed by r_{α}. The final autogenous shrinkage value depends on the water–cement ratio, expressed by $r_{\epsilon w}$, and on the cement type, expressed by $\epsilon_{au,cem}$. Table 1 provides a summary of the correction factors grouped by admixture combinations and arranged according to the magnitude of the effect on shrinkage. The governing scaling parameters are those on top of the table.

8 Combination of autogenous and drying shrinkage

At the stripping of the mold and start of drying exposure, some autogenous shrinkage and self-desiccation (i.e., a reduction of pore humidity) has already taken place. Thus, the humidity difference between the pores and the environment is reduced. This causes a reduction of apparent shrinkage, which is relevant in specimens of high-strength concretes but not normal concretes, in which the self-desiccation is insignificant. Therefore, the drying shrinkage tests of high strength concretes must

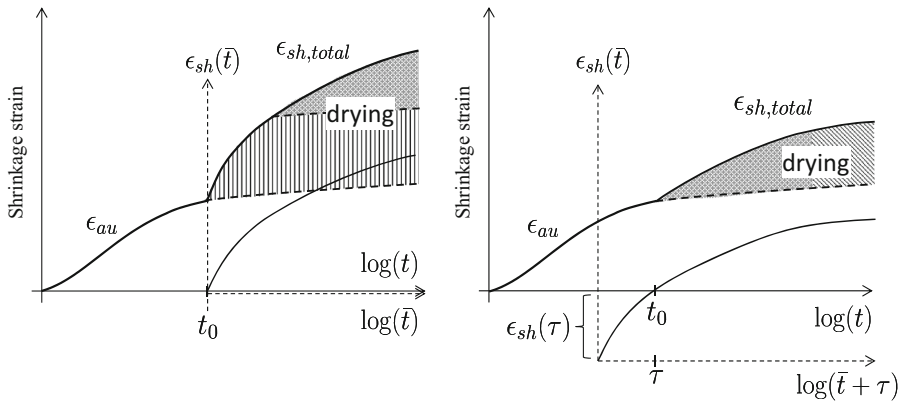

Fig. 2 Illustrations of different additive rules considered for the inclusion of autogenous shrinkage; **a** without interaction with drying shrinkage, **b** considering delayed drying shrinkage due to the early autogenous shrinkage humidity drop

(a) Additive combination without interaction

$$\epsilon_{au}(t) + \epsilon_{sh}(t - t_0)$$

(b) Additive combination with interaction

$$\epsilon_{au}(t) + \epsilon_{sh}(t - t_0 + \tau) - \epsilon_{sh}(\tau)$$

include measurement of the autogenous shrinkage prior to drying exposure. Unfortunately, most data in the database miss this information.

The autogenous shrinkage must actually have two distinct sources: (a) the volume decrease of calcium silicate hydrates and other compounds during the chemical reactions of hydration, and (b) the self-desiccation, i.e., the drop of pore humidity due to withdrawal of the free water from the pores needed for hydration. Were the former dominant, the total shrinkage would be the sum of drying and autogenous shrinkage, and if the latter were, the total shrinkage would approximately be the maximum of drying and autogenous shrinkage. Regrettably, there are no data for the interaction of drying and autogenous shrinkage, and almost no data on both the drying and autogenous shrinkages of the same concrete.

Since the amount of reactants is finite, it is clear that, like the drying shrinkage, the autogenous shrinkage must approach a finite asymptotic bound. Unfortunately, no test data with long enough durations exist to confirm it (this may be explained by the deplorable practice of using linear, rather than logarithmic, time scale plots, which give a false impression of approaching a bound, especially in elongated rectangular diagrams).

Most tests in the database aimed at drying shrinkage actually measured only the total (drying plus autogenous) shrinkage in drying environment and did not include separate tests of the autogenous shrinkage alone. Such tests are indispensable for determining the separate contribution of drying shrinkage, since the autogenous shrinkage continues even after stripping the mold and, in the core of specimen, is unaffected by drying for a long time (typically months), until the moment at which the drying front penetrates to the core and decreases the pore humidity to a value lower than the self-desiccation. The time to reach this moment is obviously much longer for the specimen core than for the surface layer, and depends on specimen size.

Since the database does not suffice to distinguish between the aforementioned formulae, illustrated in Fig. 2, the additive formulation in Fig. 2a has been adopted, as it is more conservative. Additionally, the superposition of both components allows for simplicity of design equations (as seen in fib Model Code 90/99 or 2010). After this formula has been identified from the database, the tests of shrinkage in a drying environment have been fitted taking into account a contribution of the autogenous shrinkage as predicted from this formula.

9 Parameter identification and optimization

The general optimization algorithm and strategy used to calibrate Model B4 are described in [2]. Compared to the calibration of creep, the sum of squared errors that is to be minimized is less sharp (or flatter), and thus the fit optimization problem is closer to ill-posedness [52]. This is because most shrinkage data do not satisfy the following two requirements: (1) To be able to identify the shrinkage halftime and the final value, the time range of the shrinkage test must be long enough for the logarithmic scale plot to flatten off and

show an approach to the final bound, and (2) to avoid the initial offset, i.e., the strain and time shift of the entire shrinkage curve, the first reading must be taken right after the stripping of the mold, preferably within a few seconds. Generally, short-term data are not enough to model the time evolution of shrinkage, and small errors in such data lead to large errors in long-time extrapolation and in the final asymptotic value [52].

A step-by-step approach, based on the fact that the shrinkage curve must initially evolve as the square root of time, was used to make corrections to the reported data for the initial offset. Furthermore, a multi-dimensional weighting scheme was used to counteract various kinds of bias which exist in the available test data, as detailed in [2].

The first step in developing the B4 equations was to study the sensitivity of various aspects of the shrinkage equation to the main composition parameters (w/c, c, a/c ,…). Once the strongest dependencies were identified and introduced into the formulae, parameters were assigned to scale their effects. To obtain the optimum model for the common concrete compositions, first the complete parameter set was optimized using only data sets for normal Portland cement with no admixtures, and for the temperature of approximately 20 °C. At the same time, the data subsets that cover the full time range were used to tune variables characterizing the shrinkage rate. The long-term data that show the full S-shaped curve in log-time were identified and assigned higher weights in the optimization phase dedicated to finding the predictor equations and scaling factors related to the final shrinkage value because they are the only ones giving information on the latter.

While each of these subsets was fitted statistically, which was done both by minimizing the coefficient of variation of errors divided by the data mean (C.o.V.) and the correlation coefficient R^2, the individual curve in a broad-range had to be checked visually and by statistics of individual curves to ensure that a statistically 'good' overall fit would indeed capture the correct log-scale S-shape of the shrinkage curve. Once the final parameter set for the average mix composition was determined, a different set of scaling parameters was introduced for each deviation from the average composition (e.g., for different cement types or admixtures). The location of the scaling factors was based on considering the known effect of the additive type on the microstructure or the hydration process.

The scaling factors were optimized to data subsets giving information on the cement types, temperature ranges, admixture types and, lastly, aggregate types. Factors whose influence on the quality of fit turned out to be less than the rounding accuracy were considered constant, to simplify the model, even if a slight dependence was expected and seen to exist.

As an example, consider how shrinkage depends on the aggregate type. Most data in the NU database do not specify the aggregate type. The portion of the tests that does was subdivided into categories with at least 5 tests. A literature review revealed the average values and ranges of Young's modulus, density, porosity, and moisture expansion of each aggregate type [29, 53–57]. Theoretically, the aggregate stiffness must have a restraining effect on shrinkage and the density may affect the overall permeability. A sensitivity study indicated that the shrinkage halftime was most correlated to the aggregate density and the final shrinkage value to the elastic modulus of aggregate, as seen in Fig. 3. Factors could then be introduced on these two parameters for optimization. The halftime factor was optimized to fit the S-shaped test curves of full time range, and the final value factor to fit the long-time curves. The optimized aggregate scaling factors of Model B4 are presented as a table in [1].

The optimization led to a good match of all the autogenous and drying shrinkage tests in the NU

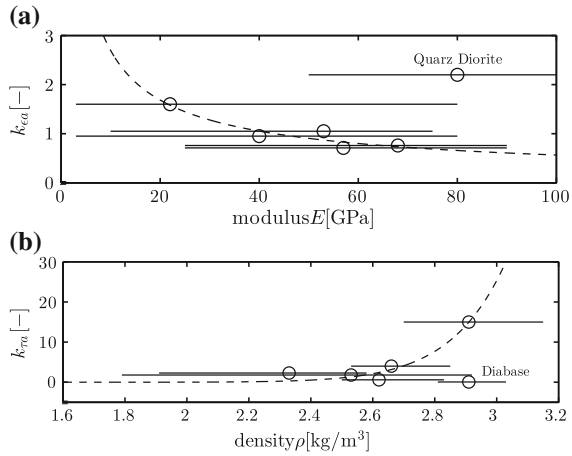

Fig. 3 Dependence of aggregate type correction factors for **a** shrinkage halftime on aggregate density, and **b** final shrinkage on aggregate modulus

database. To quantify the effect of various admixtures, by themselves and in combination, the sensitivity of the C.o.V. of errors to the model parameters has been studied. As expected, the admixtures influence primarily the autogenous shrinkage. They have only a limited effect on the drying shrinkage, in which case only the drying shrinkage halftime is affected and depends only on the cement type factor, τ_{cem}.

A number of interesting observations may be drawn from Tables 1–3. For admixture classes with insufficient data, marked by asterisk, the correction factors have been obtained by linear interpolation of calibrated neighboring values. Clearly, more systematic testing and understanding of the underlying micro-scale mechanisms is required, especially for new admixtures entering practice.

Within the presented framework, a simple optimization of the four admixture factors should be sufficient to allow the consideration of newly developed admixtures, provided that any tests needed for the optimization be performed according to the method detailed in [2].

Tables 2 and 3 list the cement type dependent parameters in the drying and autogenous shrinkage models. The rapid hardening (RS) cements reveal a substantial decrease of the shrinkage halftime, explained by accelerated hydration and hardening of the material and thus also a decreased gradient of pore humidity. The permeability of concrete further decreases due to the accelerated development of the microstructure compared to the standard cement, which further slows down the drying process.

It is also systematically observed that RS type cements cause higher amounts of shrinkage, manifested in a higher final shrinkage value. In the case of autogenous shrinkage, the rapid hardening cement may actually cause intial expansion of the cement matrix which is later counteracted by the drying shrinkage component. The slow hardening cements do not have a significant influence on autogenous shrinkage and lead to a shrinkage development similar to that of normal concretes. However, the slow hardening cements alter the dependence on the composition parameters associated with the shrinkage rate.

All the possible combinations of different cement types and admixtures create a very large parameter space. The increasing scope of potential concrete mixes, cement types, and admixtures requires increasingly complex models in design. This growing model complexity brings with it an attenuated prediction uncertainty which should be reduced, whenever possible, by updates with individual test data.

Table 2 Cement type dependent parameters for shrinkage

Parameter	*R*	RS	SL
τ_{cem}	0.016	0.080	0.010
$p_{\tau a}$	−0.33	−0.33	−0.33
$p_{\tau w}$	−0.06	−2.40	3.55
$p_{\tau c}$	−0.10	−2.70	3.80
ϵ_{cem}	360E−6	860E−6	410E−6
$p_{\epsilon a}$	−0.80	−0.80	−0.80
$p_{\epsilon w}$	1.10	−0.27	1.00
$p_{\epsilon c}$	0.11	0.11	0.11

Table 3 Cement type dependent parameters for autogenous shrinkage

Parameter	*R*	RS	SL
$\tau_{au,cem}$	1.00	41.0	1.00
$r_{\tau w}$	3.00	3.00	3.00
r_t	−4.50	−4.50	−4.50
r_α	1.00	1.40	1.00
$\epsilon_{au,cem}$	210E−6	−84.0E−6	0.00E−6
$r_{\epsilon a}$	−0.75	−0.75	−0.75
$r_{\epsilon w}$	−3.50	−3.50	−3.50

10 Uncertainty factors

For lack of deeper knowledge, it is assumed that all of the observed random deviations are caused by the inherently large composition variability. Hence, the re-scaling of all individual test curves (both horizontal and vertical) is used to estimate this composition based uncertainty in shrinkage halftime, τ_{sh}, final shrinkage, ϵ_∞, and the corresponding parameters of the autogenous shrinkage model.

The resulting histograms and derived distributions are presented in Fig. 4. Note that the empirical density function can be approximated quite well by a log-normal distribution which, in consequence, is used to provide 5 and 95 % percentiles. This uncertainty quantification provides essential input information for any form of reliability and life-time performance assessment as presented e.g. in [30–32]. The resulting asymmetrical 5 and 95 % confidence limits for the

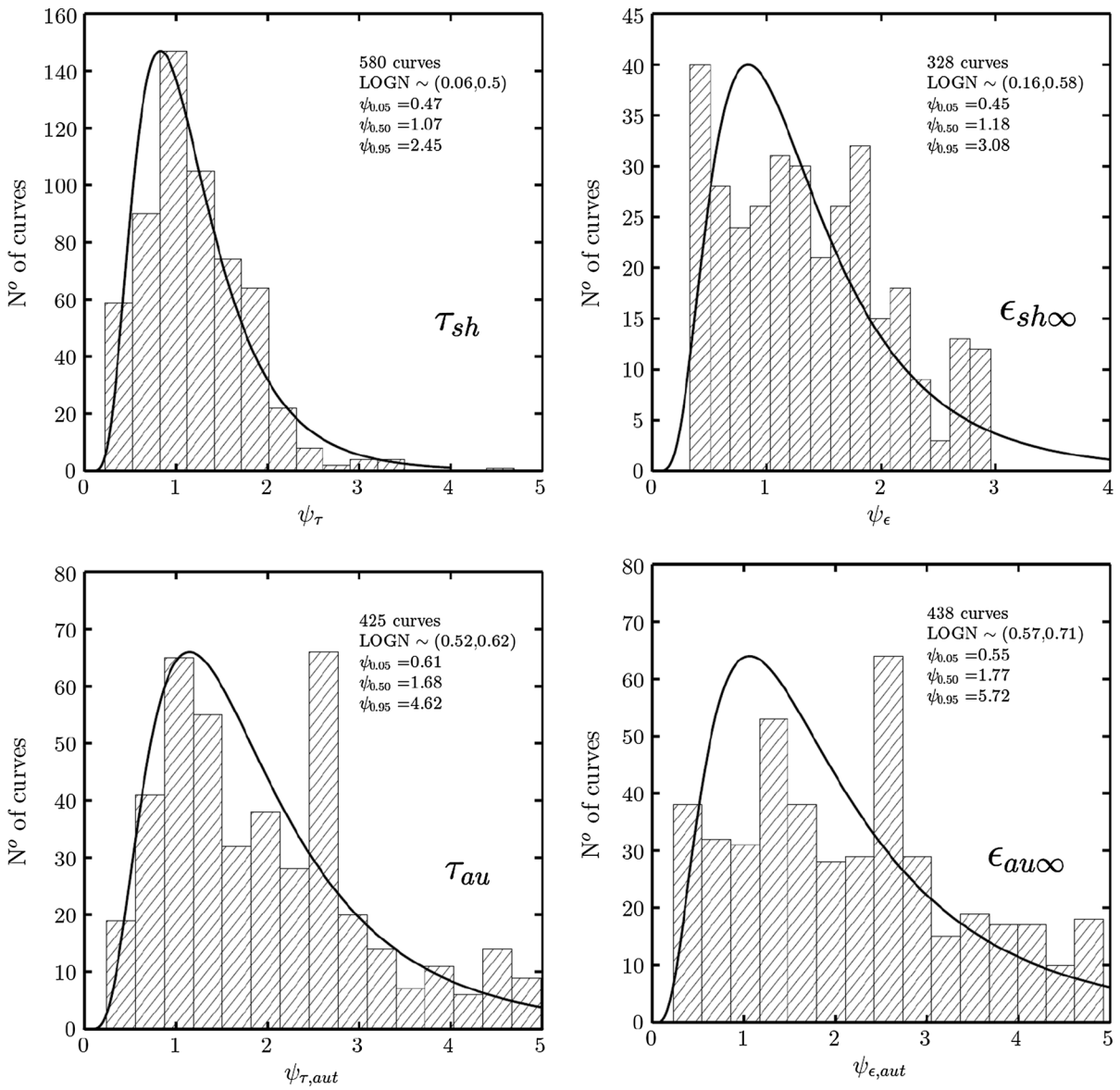

Fig. 4 Distribution of scaling factors—uncertainty quantification in model parameters

main parameters of the shrinkage model are: $\tau_{sh} \in [0.5, 2.5]$, $\epsilon_{sh,\infty} \in [0.5, 3.1]$, $\tau_{au} \in [0.6, 4.6]$, and $\epsilon_{au,\infty} \in [0.6, 5.7]$.

11 Model verification and validation

A number of statistical analyses were performed in the development of shrinkage Model B4, but only the verification, with comparisons of the final formula to the existing models [ACI, B3, GL00, MC10, MC99], is presented here. For such an analysis, it is critical to consider the capability of each model to fit the broad range of individual test curves as well as provide statistics of the overall data fit.

Among concrete researchers, it has been popular to verify and calibrate models by means of a scatter plot of the measured versus predicted values [58–60]. However, this an ineffectual statistical comparison because the statistical trends are not reflected, the

statistics are dominated by short-term measurements and old data, and the scatter due composition variability masks the scatter in the shape of time evolution curves [61]. A meaningful analysis must take into account the time function form (i.e., the capability to capture the main parameter trends with respect to the size, temperature, relative environmental humidity, and the intrinsic parameters such as composition and strength), as well as the global database statistics of the overall calibration quality.

To verify and calibrate Model B4 effectively, Figs. 5 and 8 present bar charts comparing the C.o.V. for each available model (based on subsets of the full NU database). Figures 6 and 7 present example fits of specific trends for Model B4 and the ACI 1992 model, respectively. Figure 8 presents the evolution of the C.o.V. of full database fits (in half-decade log-scale steps). Figure 9 presents the means and the symmetric 90 % confidence limits (i.e., the 5 and 95 % percentiles of the error distribution) of the distribution of fitted residuals over half-decades of data in the NU database.

The functional forms of time evolution of different models were investigated as the first step. To that end, each model was re-fitted to the individual shrinkage curves where only curves with sufficient data in both the initial range (specifically, the curves having a data point for $\leq$1 day) and the final range (approaching the horizontal asymptote) were considered. Both the autogenous and drying shrinkage models are characterized by the halftime (for horizontal scaling) and the final shrinkage value (for vertical scaling) determined from the intrinsic and extrinsic parameters. These horizontal and vertical scaling factors, depending on the model, were rescaled by factors bounded consistently in the interval [0.3, 3.0] with a starting value of 1. Only autogenous shrinkage was allowed to vary over a broader range, to account for its high uncertainty and large potential contribution. For the purpose of this statistical investigation, no correction by initial offset was applied. A model with the correct functional form would thus show the lowest overall C.o.V. while a good global calibration of the model would be indicated by low deviations from 1.

Table 4 summarizes the time functions, both for the drying shrinkage and autogenous shrinkage, the number of intrinsic parameters, and the number of fitted parameters for each model, for vertical as well as horizontal scalings (function $[t/(\alpha+t)]^{-1/2}$ was coopted from the 1978 BP Model [13] and was proposed and justified in [12]).

Only 7 individual curves satisfied the criteria for evaluating the initial shape of the shrinkage function. After applying the weights and introducing the statistical indicators from [2], the following results, shown in Fig. 5a, have been obtained. The composition based full Model B4 provides the best overall fit. The strength based Model B4 with fixed autogenous shape parameter α performs on a similar level as the *fib* model codes 1999 and 2010, followed by B3 and the Gardner–Lockman model. The ACI92 model can be refitted to represent the initial shape quite well, second only to the full Model B4.

Note that if the autogenous shrinkage of the concrete tested is likely to be high but is not reported,

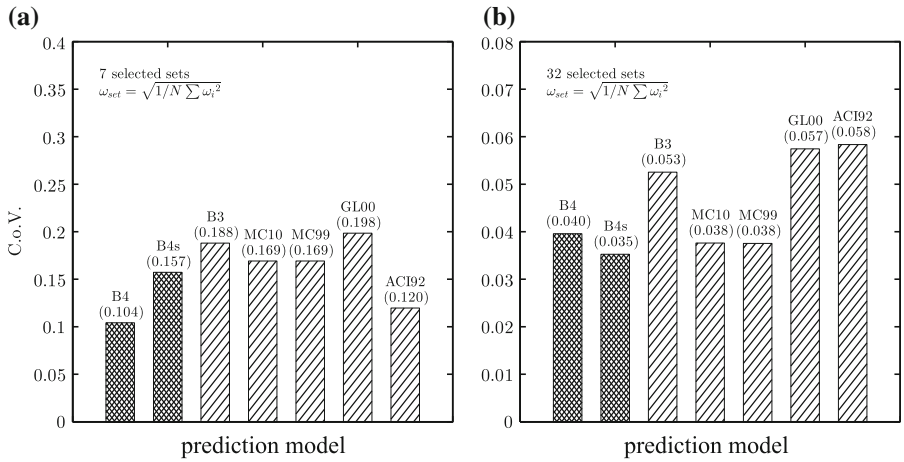

Fig. 5 Quality of fit for subsets with sufficient data in **a** initial asymptotic part of curve, and **b** final part of curve

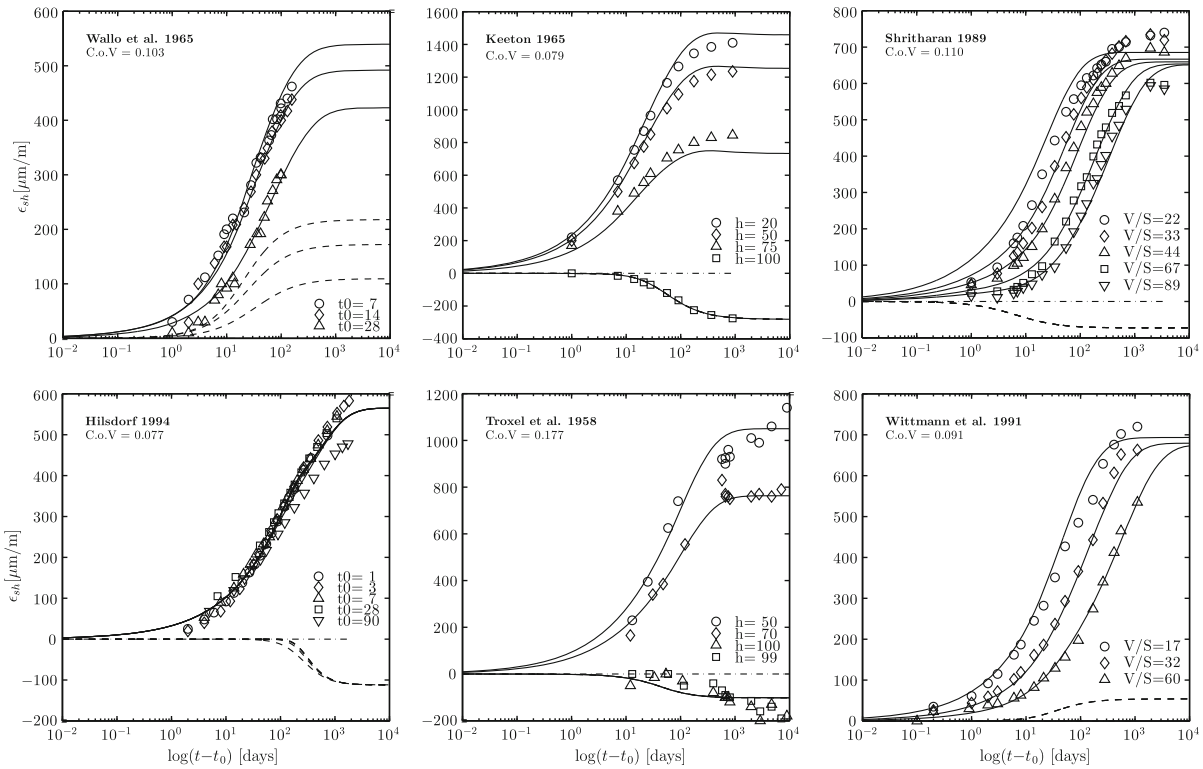

Fig. 6 Example fits of select shrinkage test curves, predicted with Model B4

then the initial shape corresponding to diffusion theory cannot be checked. The reason is that autogenous shrinkage continues in the wet core of specimen even after the drying exposure, until the drying front penetrates the core. The thicker the specimen, the longer this penetration takes. This alters the size effect on the initial shrinkage.

For comparing the terminal shape of the shrinkage function, only 32 curves that clearly approach the horizontal final asymptote have been identified; see Fig. 5b. Based on these results, it transpired that the models lacking an explicit autogenous shrinkage formulation cannot adequately represent the observed long-term shrinkage evolution. It is interesting to note that the composition dependence of the autogenous shrinkage function (captured by α) improves the data match in the initial time range but worsens it slightly in the final range.

The evaluation of the time function shape is the most basic check, which has often been ignored in the past but should always be performed for new models in the future (especially after new data illuminate the long-term autogenous shrinkage and its interaction with drying shrinkage). The functional form of the shrinkage curves aside, the capability to predict the effect of variations in the extrinsic and intrinsic parameters is the check second in importance.

Only physically based formulations can be trusted to be predictive in extrapolations, as exemplified by switching from the vertical scaling in the CEB and *fib* models to the D^2 size dependence of shrinkage halftime. The example fits in Figs. 6 and 7 represent subsets of the experimental data from the NU database capturing the variation of a single parameter (particularly the time of exposure, specimen size, and relative environmental humidity) while keeping the concrete composition constant.

The predictions of both Model B4 and the ACI 1992 model were re-scaled to match the particular concrete, in an effort to make conspicuous the capabilities of the model. Analogous to the functional form investigation, a vertical scaling factor for the shrinkage magnitude and another one for the horizontal scaling through the halftime were introduced, both for the drying shrinkage function and, where applicable (B4,MC99,MC10), also for the autogenous shrinkage function. Contrary to the earlier investigation, the 4

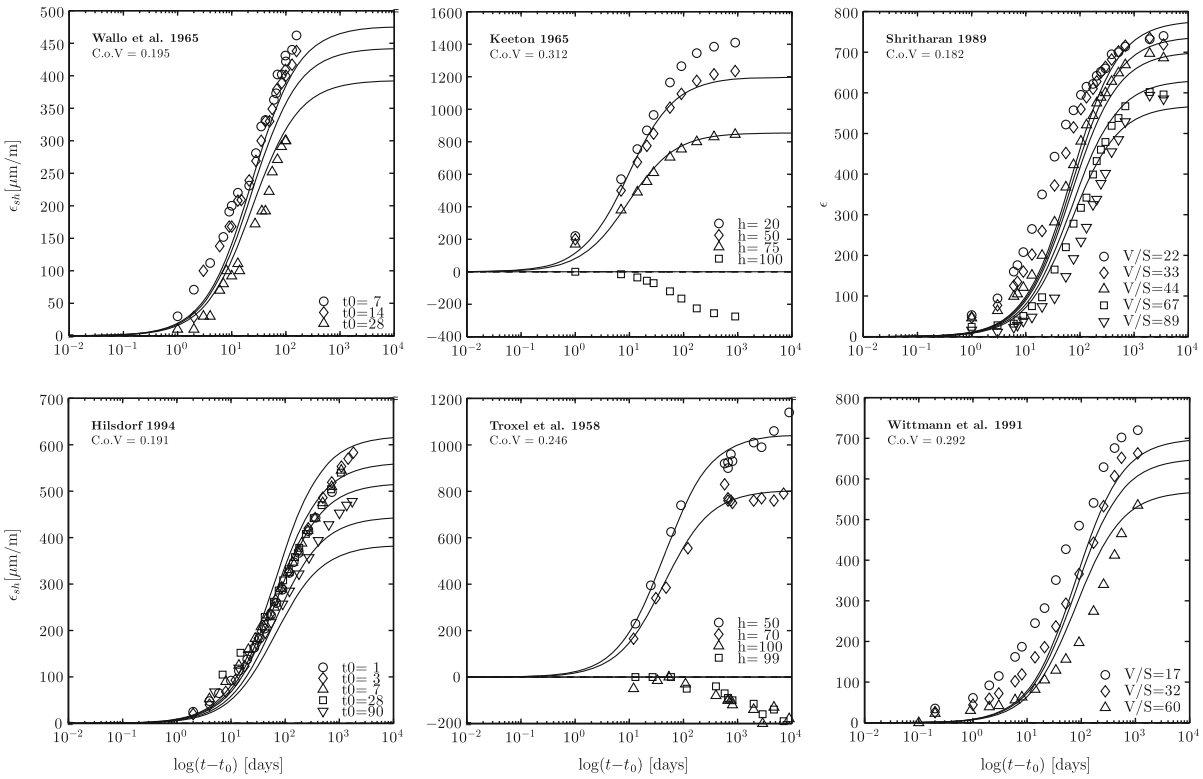

Fig. 7 Example fits of select shrinkage test curves, predicted with the ACI 1992 model

unknowns with starting value 1, bounded in [0.3,3.0], were optimized to fit the full series of curves belonging to the same concrete and a single parameter variation. Note that the majority of test data could be captured by Model B4 with a C.o.V less than 10 % on the average, but only about 20 % by the ACI 1992 model.

In total, 36 sets with clear parameter variations, such as the ones presented in Fig. 6, could be extracted from the NU database and statistically evaluated for each of the prediction models listed in Table 4. This comparison, presented in [2], confirms the high quality of the B4 shrinkage model. For all the sets and all models, a consistent set of bounds for the scaling factors was prescribed. The chosen data sets are assumed to be of good quality, without significant measurement errors.

As the third check, the overall calibration quality of all the shrinkage curves in the NU database, complying with the applicability range criteria, was compared. No re-scaling could, of course, be carried out for this check. Curves with input data insufficient for even one of the models had to be omitted. Figure 8 shows the bar charts for the C.o.V. of all shrinkage models. The statistics are computed first for the entirety of all concretes and then only for the concretes without admixtures. To obtain the corresponding evolutions of the C.o.V. value over time, the statistics were computed independently for each half-decade in $\log(t - t_0)$.

From the statistical comparisons in Fig. 8a,c, note that both B4 and GL00, the two models that have been calibrated by experiments including modern concretes, give lower C.o.V.'s in comparison to the full database. Model GL00, however, cannot capture well the shrinkage evolution in time, mainly because it lacks a separate function for autogenous shrinkage; see Fig. 5b. This function introduces important additional parameters, which allow a more accurate representation of the shrinkage curve and, of course, reflect the shrinkage mechanism more realistically. As a result, Model B4 shows the lowest C.o.V. of errors in the comparisons with the data covering both long and short times (Fig. 5), and the best overall quality of fit over the longest time range; see parts b and d of Fig. 8.

Figure 9 presents the distribution of residuals (or errors) of the shrinkage prediction at various drying

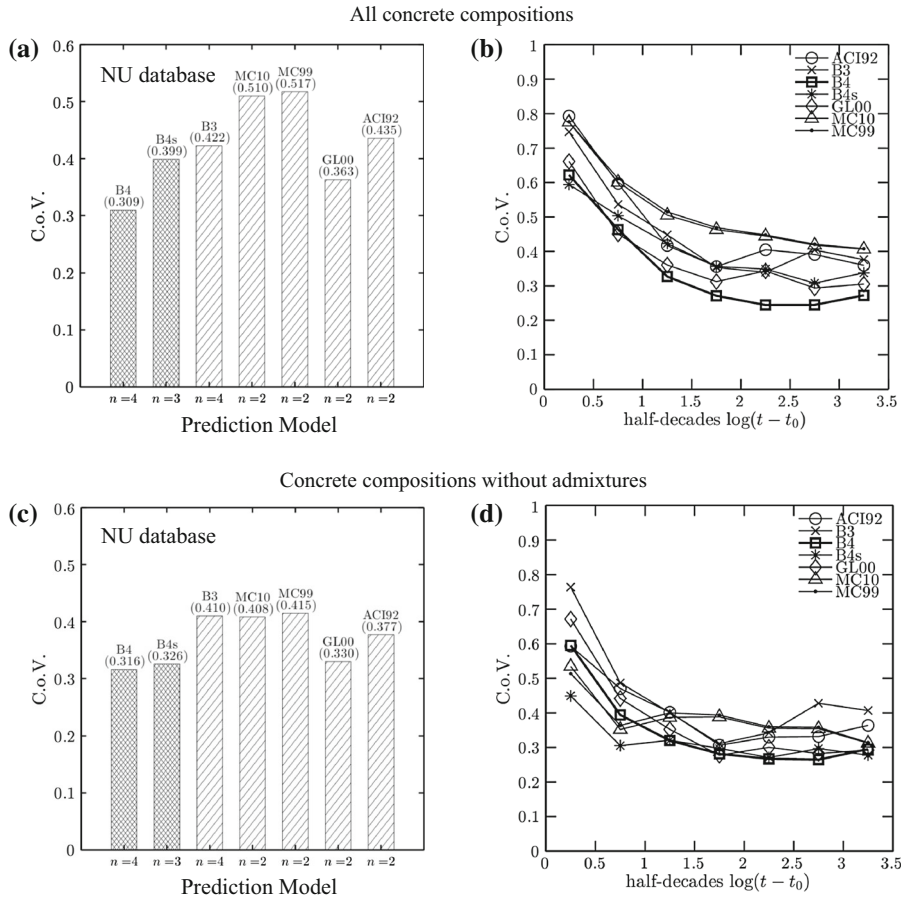

Fig. 8 Quality of fit according to the shrinkage prediction model; (**a**, **c**) total coefficient of variation of shrinkage models, (**b**, **d**) development of coefficient of variation with drying time

times. This gives a different, interesting insight, though less relevant than the C.o.V., which is what is minimized in calibration. For the first, third, fifth, and seventh half-decade, plots are also made for the best fitting theoretical distribution of residuals, used to obtain the confidence limits. The evolution of the error in the mean prediction is shown in Fig. 9 by the solid curves, and the evolution of the scatter band of 5 and 95 % percentiles is shown by the dashed curves. Model B4, as well as B4s, is overall conservative in that it presents, on average, the least underestimation through all half-decades while maintaining a relatively narrow scatter band, which is due to having optimized the model by minimizing the C.o.V. of errors rather than the errors (or residuals) per se. It shows only a small underestimation of the mean for long times. In comparison, the residuals of MC10 increase in time and, in particular, lead to a significant underestimation of long-term shrinkage, especially in the 95 % cutoff.

The ACI92 model shows the most inconsistent behavior. In the beginning, the shrinkage is underestimated, between 30 and 1,000 days it is overestimated, and ultimately tends to underestimations again. The resulting scatter band is very wide.

12 Concluding remarks

(1) Considering all the different kinds of statistics, one must conclude that, overall, Model B4 gives the best predictions.
(2) It is interesting that Model B4s, which considers the compression strength rather than the composition, performs almost as well as B4. It,

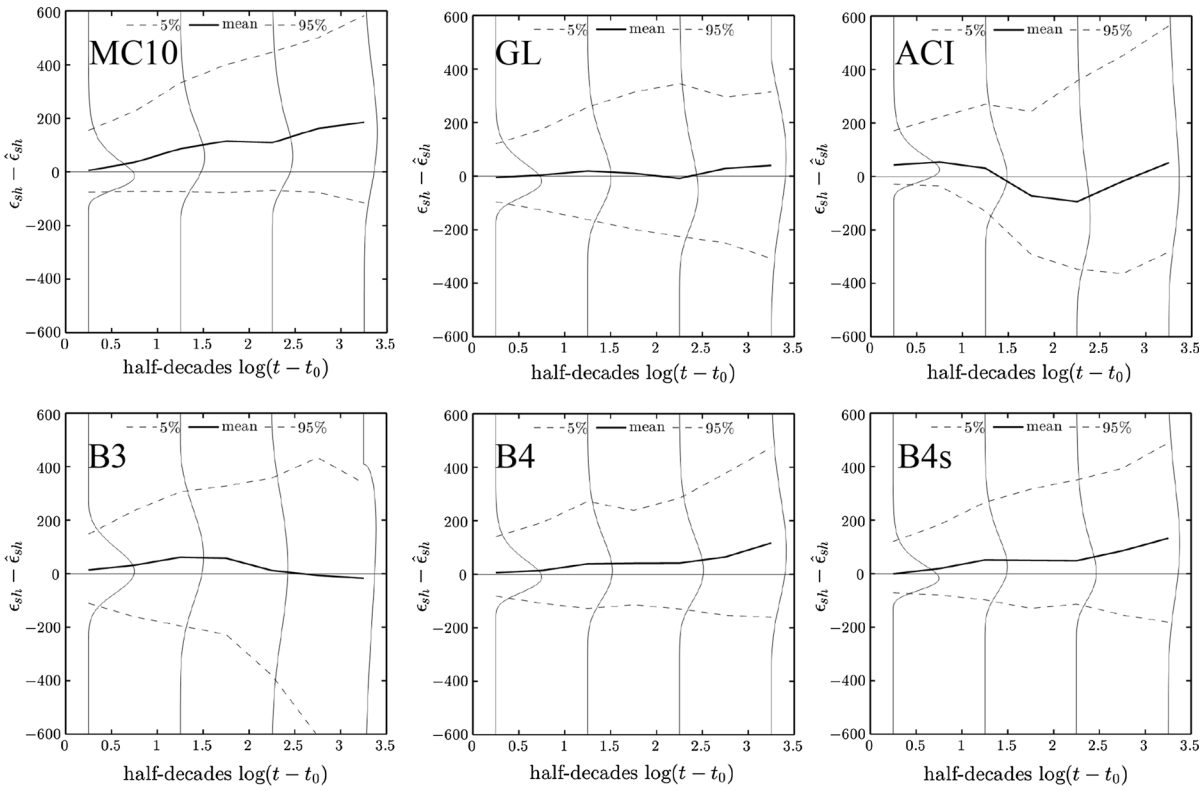

Fig. 9 Distribution of residuals with drying time according to shrinkage prediction models

Table 4 Summary of time functions and parameters of various shrinkage models and the corresponding number of intrinsic parameters and fitted parameters used for the model comparisons

Model	Time function	Autogenous time function	Intrinsic parameters	Fitted parameters
B4	$\tanh\sqrt{t/\tau_{sh}}$	$\left[1+\left(\frac{\tau_{au}}{t}\right)^{\alpha}\right]^{-r_t}$	4	4
B4s	$\tanh\sqrt{t/\tau_{sh}}$	–	3	2
B3	$\tanh\sqrt{t/\tau_{sh}}$	–	4	2
MC10	$\sqrt{\frac{t}{\tau_{sh}+t}}$	$1-e^{-\tau_{au}\sqrt{t}}$	2	4
MC99	$\sqrt{\frac{t}{\tau_{sh}+t}}$	$1-e^{-\tau_{au}\sqrt{t}}$	2	4
GL00	$\sqrt{\frac{t}{\tau_{sh}+t}}$	–	2	2
ACI92	$\frac{t^{\psi}_{sh}}{f+t^{\psi}_{sh}}$	–	2	2

however, lacks the capabilities to predict the influence of composition under the presence of admixtures, which is essential in the design phase of critical applications.

(3) Inclusion of the autogenous shrinkage of high strength concretes is crucial and is one of the main improvements over Model B3. So are the scaling parameters introduced here to capture the effects of admixtures and aggregate type.

(4) Since the ACI-209 model [4] has remained virtually unchanged since 1971, it is no surprise that it appears to be the worst.

(5) In spite of great effort, the scatter of predictions on a cross-section level is still large, and probably cannot be improved much. The main reason is that the current design practice demands predictions of the mean shrinkage in the cross section of long members, which allows

one- or two-dimensional structural analysis. A constitutive, i.e., point-wise, model for concrete (as a smoothing continuum) would probably be much simpler and would probably exhibit much less random scatter. But it would require three-dimensional analysis of stresses, cracking, hydration progress, and water diffusion in structures, as well as in test specimens. Further scatter stems from the increasingly more complex interactions of chemical reactions on the micro-scale that can only be empirically captured on the macro-scale.

(6) It is, therefore, essential to update the predictions from short-time tests of both drying and autogenous shrinkage of the given concrete. Such update requires either measuring the simultaneous water loss and the final water loss upon heating after the end of test, as described in [7], or conducting a companion shrinkage test on a much smaller specimen, or both [62]. The water loss, unfortunately, could not be included in the database, since only two papers reported such data. Same as in 1995, it is again recommended to future experimenters to always include the water loss measurements, or measurements of shrinkage on much smaller companion specimens, or both [62].

Acknowledgments Generous financial support from the U.S. Department of Transportation, provided through Grant 20778 from the Infrastructure Technology Institute of Northwestern University, is gratefully appreciated. So is an additional support under U.S. National Science Foundation grants CMMI-1129449 and CMMI-1153494 to Northwestern University. Thanks are also due for additional financial support by the Austrian Federal Ministry of Economy, Family and Youth and the National Foundation for Research, Technology and Development and from the Austrian Science Fund (FWF) in the form of Erwin Schrödinger Scholarship J3619-N13 granted to the first author.

References

1. RILEM Recommendation TC-242-MDC (2014) Model B4 for creep, drying shrinkage and autogenous shrinkage of normal and high-strength concretes with multi-decade applicability. Mater Struct (accepted)
2. Wendner R, Hubler MH, Bažant ZP (2014) Optimization method, choice of form and uncertainty quantification of model B4 using laboratory and multi-decade bridge databases. RILEM Mater Struct (accepted)
3. Hubler MH, Wendner R, Bažant ZP (2014) Comprehensive database for concrete creep and shrinkage: analysis and recommendations for testing and recording. ACI (accepted)
4. ACI Committee 209 (2008) Guide for modelling and calculating shrinkage and creep in hardened concrete. ACI Report 209.2R-08, Farmington Hills
5. FIB (1999) Structural concrete: textbook on behaviour, design and performance, updated knowledge of the CEB/FIP Model Code 1990, vol 1. Bulletin No. 2. Fédération internationale du béton (FIB). Lausanne, pp 35–52
6. FIB (2010) Model Code 2010. Fè dè ration internationale de béton, Lausanne
7. Bažant ZP, Baweja S (1995) Creep and shrinkage prediction model for analysis and design of concrete structures: Model B3. RILEM Recommendation. Mate Struct 28:357–367 (Errata, 29, p. 126)
8 Gardner NJ (2000) Design provisions of shrinkage and creep of concrete. In: Al-Manaseer A (ed) Adam Neville symposium: creep and shrinkage—structural design fffect. American Concrete Institute, Farmington, pp 101–104
9. Gardner NJ, Lockman MJ (2001) Design provisions of shrinkage and creep of normal-strength concrete. ACI Mater J 98(2):159–167
10. Wendner R, Hubler MH, Bažant ZP (2014) Statistical justification of Model B4 for multi-decade concrete creep and comparisons to other models using laboratory and bridge databases. RILEM Mate Struct (accepted)
11. Bažant ZP, Najjar LJ (1972) Non-linear water diffusion in non-saturated concrete. Mater Struct (RILEM, Paris), 5:3–20
12. Bažant ZP, Osman E, Thonguthai W (1976) Practical formulation of shrinkage and creep in concrete. Mater Struct 9:395–406
13. Bažant, ZP, Panula L (1978) Practical prediction of time-dependent deformations of concrete. Mater Struct (RILEM, Paris) 11:307–316, 317–328, 415–424
14. Bažant ZP, Yu Qiang, Li Guang-Hua (2012) Excessive long-time deflections of prestressed box girders: I. Record-span bridge in Palau and other paradigms. ASCE J Struct Eng 138(6):676–686
15. Bažant ZP, Kim Jin-Keun, Jeon Sang-Eun (2003) Cohesive fracturing and stresses caused by hydration heat in massive concrete wall. J Eng Mech ASCE 129(1):21–30
16. Wischers G, Dahms G (1977) Kriechen von frühbelasteten Beton mit hoher Angangsfestigkeit. Beton H2:69–74; H3:104–108
17. Keeton JR (1965) Study of creep in concrete. Technical reports R333-I, R333-II, R333-III. U.S. Naval civil engineering laboratory, Port Hueneme
18. L'Hermite RG, Mamillan M, Lefèvre C (1965) Nouveax résultats de recherches sur la déformation et la rupture du béton. Ann Inst Tech Bat Trav Publics 18:207–208
19. Wittmann FH, Bazant ZP, Alou F, Kim JK (1987) Statistics of shrinkage test data. Cem Concr Aggreg ASTM 9(2):129–153
20. Wallo EM, Yuan, RL, Lott JL, Kesler CE (1965) Sixth progress report on prediction of creep in structural concrete from short time tests. T & AM Report No. 658, Department of Theoretical and Applied Mechanics, University of Illinois at Urbana

21. Troxell GE, Raphael JE, Davis RW (1958) Long-time creep and shrinkage tests of plain and reinforced concrete. Proc ASTM 58:1101–1120
22. Mamillan M (1969) Evolution du fluage et des proprietes du beton. Ann Inst Tech Bat Trav Publics 21:1033, and 13; 1017–1052
23. Pentala V, Rautanen T (1990) Microporosity, creep and shrinkage of high-strength concrete. In: Heston WT (ed) ACI SP 121–21, 2nd international symposium on high-strength concrete, pp 409–432
24. England G, Ross AD (1962) Reinforced concrete under thermal gradients. Mag Concr Res 14(4):5–12
25. Ayano T, Sakata K (1997) Concrete shrinkage strain under the actual atmosphere. Proc Jpn Concr Inst 19(1):709–714
26. Jensen OM, Hansen PF (1999) Influence of temperature on autogeneous deformation and relative humidity change in hardening cement paste. Cem Concr Res 29:567–575
27. Shritharan S (1989) Structural effects of creep and shrinkage on concrete structures. M.E. thesis, Civil Engineer, University Auckland
28. Yang Y, Sato R, Kawai K (2005) Autogeneous shrinkage of high-strength concrete containing silica fume under drying at early ages. Cem Concr Res 35:449–456
29. Alexander MG (1996) Aggregates and the deformation properties of concrete. ACI Mater J 93(6):569–577
30. Strauss A, Wendner R, Bergmeister K, Costa C (2013) Numerically and experimentally based reliability assessment of a concrete bridge subjected to chloride induced deterioration. J Infrastruct Syst 19(2):166–175
31. Wendner R, Strauss A, Guggenberger T, Bergmeister K, Teply B (2010) Approach for the assessment of concrete structures subjected to chloride induced deterioration. Beton- und Stahlbetonbau 105(12):778–786
32. Strauss A, Hoffmann S, Wendner R, Bergmeister K (2009) Structural assessment and reliability analysis for existing engineering structures, applications for real structures. Struct Infrastruct Eng 5(4):277–286
33. Brooks JJ, Wainwright PJ, Neville AM (1979) Time-dependent properties of concrete containing a superplasticizing admixture. ACI J 62:293–314
34. Brooks JJ (2001) Elasticity, creep, and shrinkage of concretes containing admixtures. ACI J 194:283–360
35. Brooks JJ, Megat Johari MA (2001) Effect of metakaolin on creep and shrinkage of concrete. Cem Concr Compos 23:495–502
36. Brooks JJ (1999) How admixtures affect shrinkage and creep. Concr Int 21(4):35–38
37. Wei Y, Hansen W, Biernacki JJ, Schlangen E (2011) Unified shrinkage model for concrete from autogenous shrinkage test on paste with and without ground-granulated blast-furnace slag. ACI Mater J 108(1):13–20
38. Haque MN (1996) Strength development and drying shrinkage of high-strength concretes. Cem Concr Res 18(5):333–342
39. Tazawa EI, Miyazawa S (1995) Influence of cement and admixture on autogenous shrinkage of cement paste. Cem Concr Res 25(2):281–287
40. Persson B (1997) Long-term effect of silica fume on the principal properties of low-temperature-cured ceramics. Cem Concr Res 27(11):1667–1680
41. Bloom R, Bentur A (1995) Free and restrained shrinkage of normal and high-strength concretes. ACI Mater J 92(2):211–217
42. Igarashi SI, Bentur A, Kovler K (2000) Autogenous shrinkage and induced restraining stresses in high-strength concretes. Cem Concr Res 30(11):1701–1707
43. Jensen OM, Hansen PF (1996) Autogenous deformation and change of the relative humidity in silica fume-modified cement paste. ACI Mater J 93(6):539–543
44. Buil M, Acker P (1985) Creep of a silica fume concrete. Cem Concr Res 15(3):463–466
45. De Larrard F, Bostvironnois JL (1991) On the long-term strength losses of silica-fume high-strength concretes. Mag Concr Res 43(155):109–119
46. Termkhajornkit P, Nawa T, Nakai M, Saito T (2005) Effect of fly ash on autogenous shrinkage. Cem Concr Res 35(3):473–482
47. ACI 212 Committee (1986) Admixtures for concrete. ACI 212–1R-81, ACI 212–2R-81. ACI, Farmington
48. Jonasson JE, Hedlund H (2000) An engineering model for creep and shrinkage in high performance concrete. In: Reunion Internationale des Laboratoires D'essais et de Recherches sur les Materiaux et les Constructions (RILEM) proceedings, shrinkage of concrete, shrinkage, pp 507–529
49. Miyazawa S, Tazawa E (2001) Prediction model for shrinkage of concrete including autogenous shrinkage. In: Ulm F-J, Bazant ZP, Wittmann FH (eds) Creep, shrinkage and durability mechanics of concrete and other quasi-brittle materials. Elsevier, New York, pp 735–740
50. RILEM TC 119-TCE (1997) Avoidance of thermal cracking in concrete at early ages. Mater Struct 30(202):451–464
51. Du Beton FI (1990) Structural concrete. Textbook on behavior, design and performance—updated knowledge of the CEB/FIP Model Code 1999, vol 1–3. Federation Internationale du Béton (FIB), Lausanne
52. Bažant ZP, Xi Y, Baweja S (1993) Improved prediction model for time-dependent deformations of concrete: Part 7—short form of BP-KX model, statistics and extrapolation of short-time data. Mater Struct 26(164):567–574
53. Zhou FP, Lydon FD, Barr BIG (1995) Effect of coarse aggregate on elastic modulus and compressive strength of high performance concrete. Cem Concr Res 25(1): 177–186
54. Neville AM (1963) Properties of concrete, 4/E. Pearson Education, Singapore
55. Fossen H (2010) Structural geology. Cambridge University Press, Cambridge
56. Grübel P, Weigler H, Karl S (2001) Handbuch für Beton-, Stahlbeton- und Spannbetonbau, pp 68, 226
57. Goodman RE (1989) Introduction to rock mechanics, 2nd edn. Wiley, New York
58. Al-Manaseer A, Lam JP (2005) Statistical evaluation of shrinkage and creep models. ACI Mater J 102(3):170–176

59. McDonald DB, Roper H (1993) Accuracy of prediction models for shrinkage of concrete. ACI Mater J 90(3): 265–271
60. Al-Manaseer A, Lakshmikantan S (1999) Comparison between current and future design code models for creep and shrinkage. Revue française de génie civil 3(3–4):39–59
61. Bažant ZP, Li G-H (2008) Unbiased statistical comparison of creep and shrinkage prediction models. ACI Mater J 105(6):610–621
62. Bazant ZP, Donmez A (2015) Extrapolation of short-time drying shrinkage tests based on easured diffusion size effect: concept and reality. Mater Struct (in press)